

**OPERATIONAL EXPERIENCE WITH OPTICAL MATCHING  
IN THE SLC FINAL FOCUS SYSTEM\***

P. BAMBADE,<sup>a</sup> P. BURCHAT,<sup>b</sup> D. BURKE, W. FORD,<sup>c</sup>  
C. HAWKES,<sup>d</sup> W. KOSKA,<sup>e</sup> W. KOZANECKI, T. LOHSE, T. MATTISON,  
N. PHINNEY, M. PLACIDI,<sup>f</sup> D. RITSON, S. WAGNER<sup>c</sup>  
*Stanford Linear Accelerator Center, Stanford University, Stanford, CA 94309*

**ABSTRACT**

In the SLC Final Focus System, all components of transverse phase-space and the couplings between them must be controlled to minimize the beam size at the interaction point. After summarizing the experimental algorithm and the on-line tuning programs, we present a consistent set of measurements and describe our present understanding of the various contributions to this beam size.

*Submitted to Nuclear Instruments and Methods*

---

*Present addresses:*

<sup>a</sup>Laboratoire de l'Accélérateur Linéaire, Bât. 200, Orsay, France 91405

<sup>b</sup>University of California, Santa Cruz, CA 95064.

<sup>c</sup>University of Colorado, Boulder, CO 80309.

<sup>d</sup>California Institute of Technology, Pasadena, CA 91125.

<sup>e</sup>University of Michigan, Ann Arbor, MI 48109.

<sup>f</sup>CERN, CH-1211, Geneva, 23, Switzerland

\*Work supported in part by Department of Energy contracts DE-AC03-76SF00515, DE-AC02-76ER01112, DE-AC02-86ER40253, DE-AC03-81ER40050 and DE-AM03-76SF00010, and in part by the University of Colorado and the Max Kade Foundation.

## 1. Introduction

The Final Focus System [1] (FFS) is the last section of beam-line in the Stanford Linear Collider (SLC) before the interaction point (IP). Its main function is to maximize the luminosity by focusing the beam to the smallest possible size. Because the beam has a finite emittance and energy spread, a nominal beam size of  $2 \mu\text{m}$  at the IP can only be achieved with elaborate optics where higher order aberrations are carefully minimized [2]. In operation the FFS must also be *tunable* to absorb focusing errors accumulated in the transport lines upstream and in the FFS itself [3]. Effects from such errors manifest themselves primarily as linear mismatches between the transverse phase-space of the injected beam and the FFS optics, and must be corrected before the final focusing works properly. An experimental tuning algorithm has been developed [3] to achieve these corrections, and extensive operational experience has been acquired [4].

Initially it was thought that this tuning would be used as an overall correction for mismatches accumulated in the entire SLC, or at least in the Arcs: except for a few special cases, it is possible in principle to absorb optical distortions of up to a factor of four [3]. It was also thought that variations would be tuned continuously in the FFS. Neither appears to be feasible. Elimination of backgrounds [5] in the detector from electromagnetic debris and muons produced when beam-tails strike aperture limits upstream of the matching elements requires a nearly matched phase-space at injection. Thus major mismatches must be corrected upstream, and in practice only small adjustments are made in the FFS. The main limitations to continuous optical feedback are lack of orthogonality in the corrections and the fact that the only place available to diagnose all the distortions is the higher order corrected focal point at the IP. As a result of non-orthogonality, even modest variations in the incoming phase-space can require extensive retuning. These weaknesses result from *adding-on* the optical and background tuning strategies to a design where the basic architecture was already fixed, and suffered from severe space limitations.

Operationally, the optical tuning has evolved towards determining a stable set-up. Partly because the linac emittance presently exceeds the design value by a factor of about three in the horizontal plane [6], the optics must be configured with a larger than optimal  $\beta$ -function at the IP ( $\beta^*$ ), in order to reduce backgrounds generated in the last quadrupoles by the beam tails. The larger  $\beta^*$  and linac emittance limit the attainable luminosity. Phase-space parameters are monitored routinely to distinguish stable changes from spurious ones, and to base corrections on time-averaged quantities. After reviewing the optics, the tuning strategy and the on-line programs used, we describe measurements made with the electron beam in the last run (September 1988). Similar results have been obtained with the positron beam.

## 2. Summary of optics

The FFS consists of four telescopic modules (fig. 1). Optical demagnification is achieved in the first and final telescopes, which straddle a chromatic correction section where the intrinsic first-order chromaticity of the beam-line is compensated. The Arc lattice  $\eta$ - and  $\beta$ -functions are matched in the  $\eta$ -match section and in the first telescope, respectively.

The optimization of the chromatic correction is the central point of the design [2]. The Chromatic Correction Section (CCS) consists of two  $-I$  telescopes, combined with dipoles at the foci, to generate significant energy dispersion at the quadrupoles. Sextupoles, where the focusing strength varies linearly with excursion, are put near the quadrupoles to provide additional focusing proportional to energy. This allows cancellation of the intrinsic first-order chromaticity. Additional first-order perturbations to the imaging produced by each sextupole are made to cancel over the length of the CCS by appropriate symmetries. In this way, all residual perturbations are pushed to second-order. The effective  $\beta^*$  can thus be written:

$$\beta_{eff}^* \simeq \beta^* + \kappa_1^2 \frac{\delta_E^4}{\beta^*} + \kappa_2^2 \frac{\epsilon \delta_E^2}{\beta^{*2}} + \kappa_3^2 \frac{\epsilon^2}{\beta^{*3}} \quad , \quad (1)$$

where  $\kappa_{1,2,3}$  measure the magnitudes of the residual second-order chromatic and geometric perturbations,  $\epsilon$  is the emittance, and  $\delta_E$  is the fractional energy spread.

The effect of the chromatic correction is to broaden the energy band-pass over which rays are imaged to the same IP focal point. The width of this band-pass scales roughly as  $\sqrt{\beta^*}$  (if only the term in  $\kappa_1$  from (1) is used) [2]. Defining it quantitatively as the band of energy deviations for which  $\beta_{eff}^* \leq 1.25\beta^*$ , it is  $\pm 0.5\%$  for  $\beta^* = 16$  mm, and  $\pm 0.22\%$  for  $\beta^* = 4$  mm. Without chromatic correction, it is less than  $\pm 0.05\%$  in both cases (fig. 2).

### 3. Correction scheme

We describe the four-dimensional transverse phase-space with the usual [7] beam-matrix  $\sigma$ , where  $\sigma_{ij} = \langle x_i x_j \rangle$ . The matrix  $\sigma$  has eight free terms if the emittances  $\epsilon_x$  and  $\epsilon_y$  are set. With the four dispersion functions  $\eta_x, \eta_{x'}, \eta_y$  and  $\eta_{y'}$ , we thus need twelve parameters to describe an arbitrary optical mismatch. For the SLC, equal emittances  $\epsilon_x = \epsilon_y$  are specified. In this case, two of the four cross-plane coupling correlations— $\sigma_{31}, \sigma_{41}, \sigma_{32}, \sigma_{42}$ —are redundant [8]. With the condition  $\sigma_{21} = \sigma_{43} = 0$  at the IP, this redundancy takes the form  $\sigma_{31} = \sigma_{42}$  and  $\sigma_{32} = -\sigma_{41}$ .

The tuning strategy is designed for this case and thus involves ten corrections. It can be shown that the maximum luminosity reduction factor, which results in the case of unequal emittances from correcting only these ten distortions, is close to  $4r/(1+r)^2$ , where  $r$  is the ratio of the smaller to the larger emittance [8]. The reduction can become severe for  $r < 1/4$ .

The distortions are best characterized by what matters physically at the IP:

1. Five correlations of positions to angles and energy:  $\sigma_{21}, \sigma_{43}, \sigma_{32} = -\sigma_{41}, \eta_x$  and  $\eta_y$ , corresponding respectively to longitudinal offsets of the waists in both planes at the IP (we refer to these as offsets of the *in-plane* waists), cross-plane coupling (by analogy we refer to this as an offset of the *out-of-plane* waist), and residual spatial dispersion. The waists must be positioned to within some fraction of the depth of focus  $\beta^*$  of the demagnifying optics, and the dispersion  $\eta$  must be tuned to less than  $\sqrt{\epsilon\beta^*}/\delta_E$  to avoid dominating the final spot size.
2. Five terms affecting the angular spread at the IP:  $\sigma_{22}, \sigma_{44}, \sigma_{31} = \sigma_{42}, \eta_{x'}$  and  $\eta_{y'}$ , determine the band-pass of the optics. This is illustrated in fig. 3, which shows the luminosity  $L$  versus  $\beta^*$  for an energy spread of 0.002 ( $1/\beta^*$  is taken as a measure of the overall angular spread) [3]. If the band-pass is larger than the energy spread, linear optics dominates and  $L$  drops as  $1/\beta^*$ . If it is smaller,  $L$  is dominated by second order chromatic and geometric perturbations and drops rapidly with decreasing  $\beta^*$  [see eq. (1)]. The optimum occurs when the band-pass and energy spread are matched. For energy spreads of 0.002 now achieved [10],  $\beta_{opt}^* \simeq 4$  mm. This defines the optical limit to the luminosity.

Correction elements for the above ten distortions are shown in fig. 1. The waists are corrected with trim windings on two of the last quadrupoles just before the IP, and with a skew quadrupole just upstream. The betatron angular spread is controlled with one skew and two upright quadrupoles in the first telescope. These, combined with the waist controls, form an effective zoom-lens. Spatial and angular dispersions are corrected by perturbing the  $\eta$ -match with two pairs of upright and skew quadrupoles [11].

#### 4. Tuning strategy

The flow diagram in fig. 4 summarizes the experimental algorithm. Because each correction is coupled to the ones downstream, they must be applied sequentially.

After matching the input dispersion, the core of the program is to bring the beam to a focus at the IP in a condition such that the phase-space parameters can be correctly measured at that point. Therefore, the initial set-up has a purposely enlarged  $\beta^*$  of 30 mm, with the sextupoles tuned to suppress the first-order chromaticity. In addition to reducing backgrounds, this helps to avoid having the beam size at the IP dominated by the second order chromatic and geometric perturbations. It is also a guess of the most probable direction for the angular spread correction.

In order to decouple the final *in-* and *out-of-plane* waist adjustments (one of the angular spread corrections) the minimization of the cross-plane  $\sigma_{42}$  correlation is applied first [12]. Then the beam is brought to an initial focus by correcting the *in-plane* waists. This, if residual angular dispersion is present, and if the  $\sigma_{42}$  correlation has been imperfectly minimized, helps to diagnose residual spatial dispersion and cross-plane  $\sigma_{32}$  and  $\sigma_{41}$  correlations in the IP beam size. It thus reduces the number of iterations of waist and dispersion corrections needed to minimize the beam size. In the case of unequal emittances, the two cross-plane correlations cannot in general be simultaneously made zero. In this case, it is advantageous to set the *out-of-plane* waist correction to minimize the beam size in the plane with the smaller emittance (typically the vertical plane). Finally, to maintain the minimization of the first-order chromaticity, the sextupoles are refitted after each major optical adjustment.

After this, and unless the angular spread at the IP is too large in spite of the  $\beta^* = 3$  cm configuration, scans of the *in-plane* waists can be used to measure phase-space parameters at the IP. Inferred values of  $\beta^*$  are used to calculate angular spread corrections, and of  $\epsilon$  to compare with measurements in the rest of the machine.

## 5. - On-line matching packages

An on-line modeling and fitting package is required for dispersion and betatron angular spread corrections [13].

For *dispersion matching*, the input consists of  $\eta_x$  and  $\eta_y$  measured at chosen strip-line beam position monitors, and, optionally, at the wire targets [14] which are used to diagnose the beam at the IP. The data are obtained by recording beam motion correlated with varying the energy in the linac. The  $\eta_x$  and  $\eta_y$  values consistent with the model are determined from a fit to the measurements and give  $\eta_x, \eta_{x'}, \eta_y$  and  $\eta_{y'}$  at the entrance to the FFS. The strengths of the four correction quadrupoles in the  $\eta$ -match section are then varied to minimize the four dispersion terms at the end of the first telescope or at the IP.

For corrections to the *betatron angular spread*, the waist measurements at  $\beta^* = 3$  cm are used to specify an initial diagonal beam  $\sigma$ -matrix at the IP. The  $\sigma$ -matrix at the entrance to the FFS is calculated from the model. The six quadrupole strengths of the zoom-lens are then varied in a fit to give a new diagonalized  $\sigma$ -matrix with the desired  $\beta^*$  at the IP. To help convergence, considerable flexibility is incorporated, including multistep fitting and choice of which  $\sigma$ - and  $R$ -matrix elements to include in the  $\chi^2$  function to be minimized.

The waists are also adjusted through automated procedures, which record beam profiles measured with the wire-targets at the IP, while stepping orthogonal combinations of the two trim windings on the last quadrupoles, or the nearby skew quadrupole [15]. Estimates of  $\beta^*$  and  $\epsilon$  are obtained by fitting

$$\sigma^2 = \epsilon\beta^* + \frac{\epsilon}{\beta^*}\Delta f^2 \quad (2)$$

to the *in-plane* waist data, where  $\Delta f$  is the displacement of the waist at the IP along the beam direction. Because the squares of the beam sizes vary parabolically, the optimal correction is found, by symmetry, even if the minimum beam size is less than the wire size.

## 6. Input dispersion match

Figure 5 shows measurements of the lattice dispersion, measured in the  $\eta$ -match, First Telescope and chromatic correction sections, before and after correction. Variations serve to diagnose changes in the set-up of the Arc and are usually correctable [16]. In this figure the horizontal (upper figures) and vertical (lower figures) dispersion is shown before (left) and after (right) correction, using an example of data taken during the 1987 SLC commissioning. Note the changes in scale. In each figure the error bars on the solid curve show the results of simultaneous dispersion measurements on the electron beam using BPMs in the SLC North Arc and the  $\eta$ -matching, First Telescope and Chromatic Correction Sections of the North FFS. The solid curve is a series of straight lines joining these measurement points. The dotted curve is a series of straight lines joining points showing the corresponding value of the design dispersion at the location of each of the BPMs. After correction, the measured dispersion in the  $\eta$ -matching and First Telescope sections is very close to the design values. Such measurements are performed routinely to monitor the match. They are usually repeated to average out trajectory fluctuations during the measurement which can mimic dispersion mismatch. The match has been observed to be stable over periods of days to weeks.

## 7. Cross-plane coupling correction

Figure 6 shows the correction for the tilt in the spot on a phosphor screen near the Final Triplet (ST4 in fig. 1). A tilted spot at that point corresponds to a finite  $\sigma_{42}$  correlation at the IP. This is done manually by adjusting the skew quadrupole in the first telescope. The correction is difficult to set accurately and reproducibly because of changing beam tails and saturation effects on the screen. A fit of the  $\sigma_{13}$  correlation coefficient using the digitized profile may improve this. The available correction range is large, but the practical range is severely limited by perturbations caused to the trajectory

of the opposing outgoing beam, which must pass off-axis through the skew quadrupole before reaching the final beam dump. A procedure for controlling cross-plane coupling within the Arc has been developed, which mitigates this problem substantially [17]. Such control has reduced coupling in the lattice to about 50% and has brought the FFS skew corrections to acceptable values, although this is not fully stable and depends on the ratio of emittances at the linac exit, as described above.

## 8. Waist adjustments at the IP

Figure 7 shows an example of a waist scan (in the vertical plane). Such scans are done routinely, allowing minimum beam sizes of 3 to 5  $\mu\text{m}$  to be attained.

## 9. Dispersion corrections at the IP

There can be significant residual dispersion in the IP beam size, even after the input dispersion has been matched, due to imperfections in the FFS lattice or in the beam trajectory, or from energy-position correlations in the phase-space at the end of the linac. Dispersion from the FFS can be measured by the online package described earlier. Corrections with the four quadrupoles in the  $\eta$ -match section are practical for moderate dispersions ( $\eta_{IP} \leq 2$  mm). Larger dispersions, however, can require extreme corrector strengths which, in turn, also distort the betatron phase-space.

A complementary scheme for empirically minimizing residual spatial dispersion at the IP makes use of closed steering bumps in the chromatic correction section. Such orbit distortions generate spatial dispersion at the IP, through the first-order chromaticity of this section. For the range of interest, second-order chromatic and geometric perturbations remain small. An example of successfully applying this method to minimize the spot at the IP is shown in fig. 8. In combination with the lattice dispersions measured

in the first telescope and at the IP, this method has allowed separation of lattice dispersion generated in the Arcs and in the FFS. Since the spatial dispersion introduced by this bump to minimize the spot size has coincided with the previously measured lattice dispersion at the IP, it has been possible to put an upper limit on beam dispersion at the end of the linac.

## 10. Betatron phase-space diagnostics and adjustments at the IP

History plots of  $\epsilon$  and  $\beta^*$ , estimated from *in-plane* waist scans performed after iterating the waist and dispersion corrections to minimize the spot at the IP, are shown in fig. 9.

The emittances  $\epsilon_x$  and  $\epsilon_y$  were mostly larger than nominal and reflected, in most cases, larger than nominal values in the linac. The  $\beta^*$  values were larger than the expected optimum of  $\beta_{opt}^* \simeq 4$  mm needed to optimize the luminosity, and resulted from requiring a small enough angular spread to minimize beam tail-induced backgrounds in the last quadrupoles. In some cases, larger than nominal *effective*  $\epsilon$  and  $\beta^*$  values were also obtained because of an imperfectly corrected phase-space at the IP. The data in fig. 9 are therefore generally upper limits of actual values.

A first attempt to enlarge the (vertical) betatron angular spread is indicated by an arrow in fig. 9(d). The effect from this was clear but smaller than expected, and may have been partially offset by an upstream variation. Such adjustments will have to be iterated in order to reach the expected optimum value of  $\beta_{opt}^* \simeq 4$  mm.

The last values in the plot were obtained in the final run before the September 1988 shutdown. Dispersion at the IP generated by trajectory errors and misalignments was measured and minimized with the bump technique described above. This, and several iterations of the waist corrections, resulted in emittances close to the design value in the vertical plane and too large in the horizontal by a factor of three. This was consistent with measurements performed simultaneously at the end of the linac [6], showing that the

final beam sizes at the IP were not dominated by chromatic effects, and that the residual cross-plane coupling from the Arc did not significantly enlarge projected emittances. At that time, the linear phase-space at the IP was thus correctly estimated from these measurements.

## 11. Conclusion and prospects

The experimental algorithm developed for the FFS has enabled beams focused at the IP with 3 to 5  $\mu\text{m}$  transverse sizes to be attained, and the various contributions to the residual beam size to be diagnosed.

The residual beam size is presently limited by the larger than optimal  $\beta^*$  (dictated by detector backgrounds) and by the somewhat larger than nominal linac emittance. The reduction in luminosity from this is about an order of magnitude. In addition, a small loss in attainable luminosity arises from not fully correcting the cross-plane coupling in the case of asymmetric emittances. This loss can be up to about 25%, with the current emittance ratio of one to three.

In the next run, a new collimation system will be available at the end of the linac which, combined with the existing slits and with additional muon shielding that has been installed in the FFS tunnel, will enable beam tails to be cut more efficiently. This, coupled with progress in maintaining a nominal phase-space at the injection to the Arcs, and in reducing the  $\beta$ -function at the IP, should enable the *optical limit* to the luminosity to be reached.

## Acknowledgments

We wish to thank the very large number of people, from SLAC and elsewhere, who have helped to make all this possible. In particular, we wish to acknowledge the contributions of K. Brown, R. Erickson, T. Fieguth and J. Murray, who initiated and finalized the design of the Final Focus optics, and of L. Sweeney, who contributed to much of the control software. Fieguth and Murray also initiated the work on the experimental tuning algorithm.

We also wish to acknowledge the support and enthusiasm of our colleagues from the SLC, Mark II and Operations Groups, who helped carry through many of the measurements described here.

## References

- [1] *SLC Design Handbook*, December 1984, Stanford Linear Accelerator Center.
- [2] K. L. Brown, *A Conceptual Design of Final Focus Systems for Linear Colliders*, SLAC-PUB-4159 (June 1987).
- [3] P. S. Bambade, *Beam Dynamics in the SLC Final Focus System*, SLAC-PUB-4227 (June 1987).
- [4] P. S. Bambade, *Recent Progress at the Stanford Linear Collider*, SLAC-PUB-4610 (April 1988).
- [5] D. L. Burke *et al.*, *Beam Collimation and Detector Backgrounds at  $e^+e^-$  Linear Colliders*, these proceedings.
- [6] W. B. Atwood *et al.*, *Observation and Control of Emittance Growth in the SLC Linac*, these proceedings.
- [7] K. L. Brown *et al.*, SLAC-91, Rev. 2, May 1977.
- [8] P. S. Bambade, *Number of Dimensions of Optical Correction Space in the SLC Final Focus System*, collider note in preparation.
- [9] J. J. Murray and T. Fieguth, MURTLE, private program.
- [10] E. J. Soderstrom *et al.*, *Fast Energy Spectrum and Transverse Beam Profile Monitoring and Feedback Systems for the SLC Linac*, these proceedings.
- [11] J. J. Murray *et al.*, *The completed design of the SLC Final Focus System*, SLAC-PUB-4219 (February 1987).

- [12] P. S. Bambade, *Orthogonality of Final Waist Corrections at the IP of the SLC*, CN-369 (October 1988).
- [13] C. M. Hawkes and P. S. Bambade, *First Order Optical Matching in the Final Focus Section of the SLAC Linear Collider*, SLAC-PUB-4621 (May 1988).
- [14] D. L. Burke *et al.*, *Measurements of Cross Sectional Intensity Profiles of Beams at the  $e^+e^-$  Interaction Point of the SLC*, these proceedings, and submitted to Nuclear Instruments and Methods.
- [15] N. Phinney *et al.*, *An Automated Focal Point Positioning and Emittance Measurement Procedure for the Interaction Point of the SLC*, these proceedings.
- [16] T. H. Fieguth *et al.*, *Dispersion in the Arcs and Special Sections of the SLAC Linear Collider*, these proceedings.
- [17] P. S. Bambade *et al.*, *Wirefix — Or Harmonic Corrections in the SLC Arcs*, these proceedings.

## Figure captions

- [Fig. 1.] Schematic of the FFS. The four quadrupoles used for dispersion corrections are shown cross-hatched, and the six quadrupoles used for betatron corrections are shown shaded.
- [Fig. 2.] Optical bandpass of the FFS, with chromaticity correction (case a), and without (case b).
- [Fig. 3.] Optical luminosity versus  $\beta^*$  in the chromaticity-corrected FFS, for an energy spread  $\delta_E = 0.002$ . The curve is obtained through a simulation [9]. The approximate background limit depends on the efficacy of the collimation and shielding, and on the beam intensity.
- [Fig. 4.] Flow-diagram summarizing the application of the 10 linear optics adjustments required to minimize the IP spot.
- [Fig. 5.] The First Telescope dispersion correction.
- [Fig. 6.] Approximate correction of cross-plane coupling in the IP angular spreads, looking at the tilt in the beam shape on a screen at the high- $\beta$  point in the system.
- [Fig. 7.] Minimization of the vertical IP beam size by displacing the vertical waist with an orthogonal combination of trim windings in the last quadrupoles.
- [Fig. 8.] Correction of residual dispersion at the IP, by minimizing the spot size with a closed dispersion-generating trajectory bump in the CCS. The parameter  $x'$ KICK is the magnitude of the kick applied by a steering dipole located at the upstream end of the CCS. A corresponding dipole at the downstream end is used to close the bump.

[Fig. 9.] History plots of the emittances and  $\beta$ -functions inferred from *in-plane* waist-scans at the IP. The effect of an initial attempt towards reducing the vertical  $\beta$ -function is indicated. As can be seen, at the end of the run, emittance measurements performed simultaneously at the end of the Linac and at the IP gave consistent results.

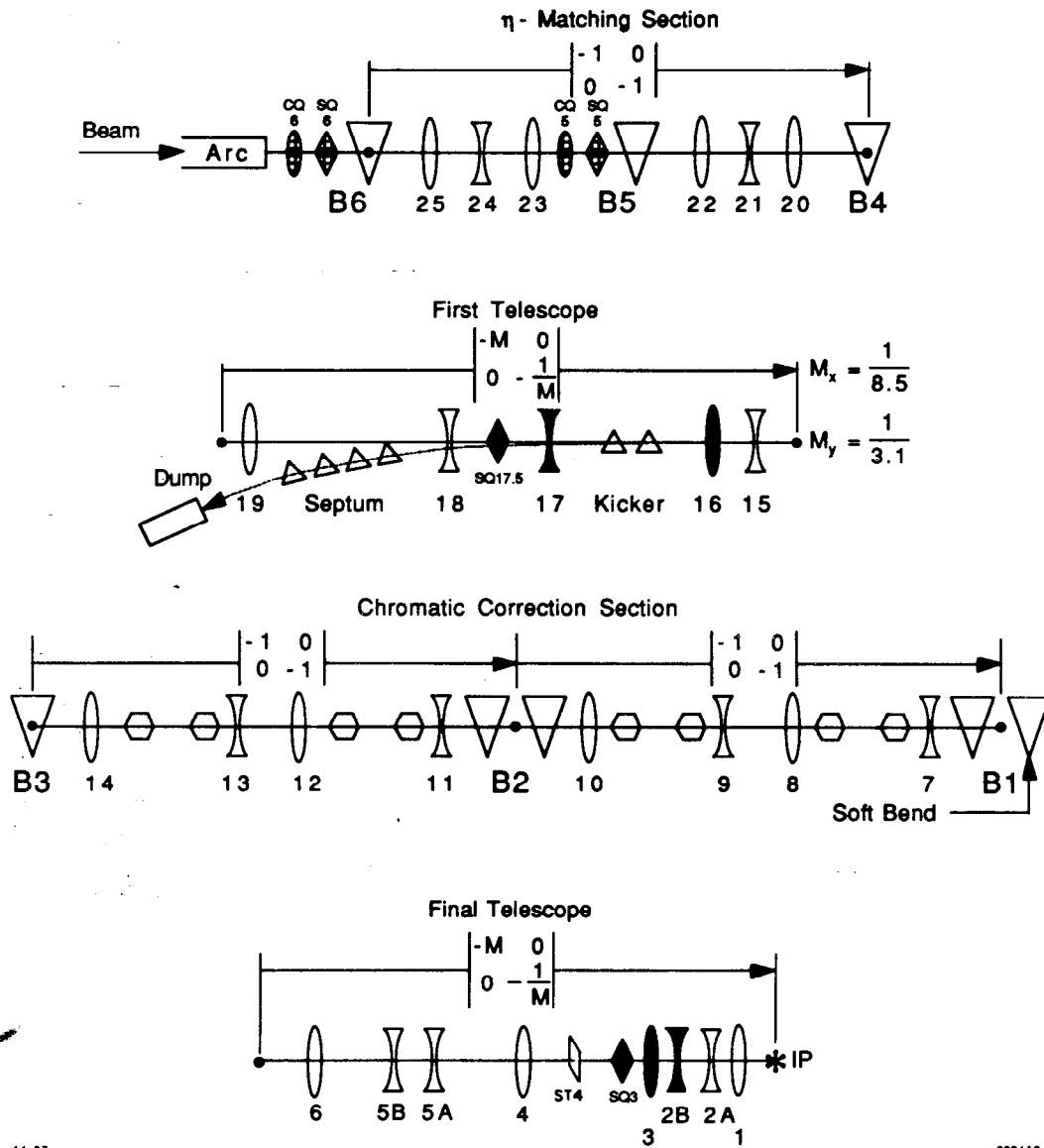


Fig. 1

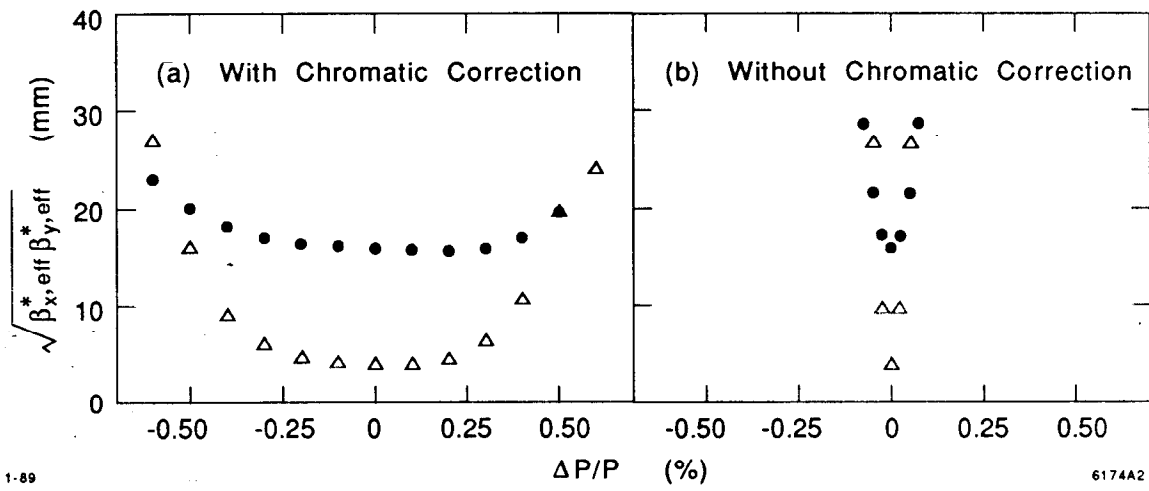
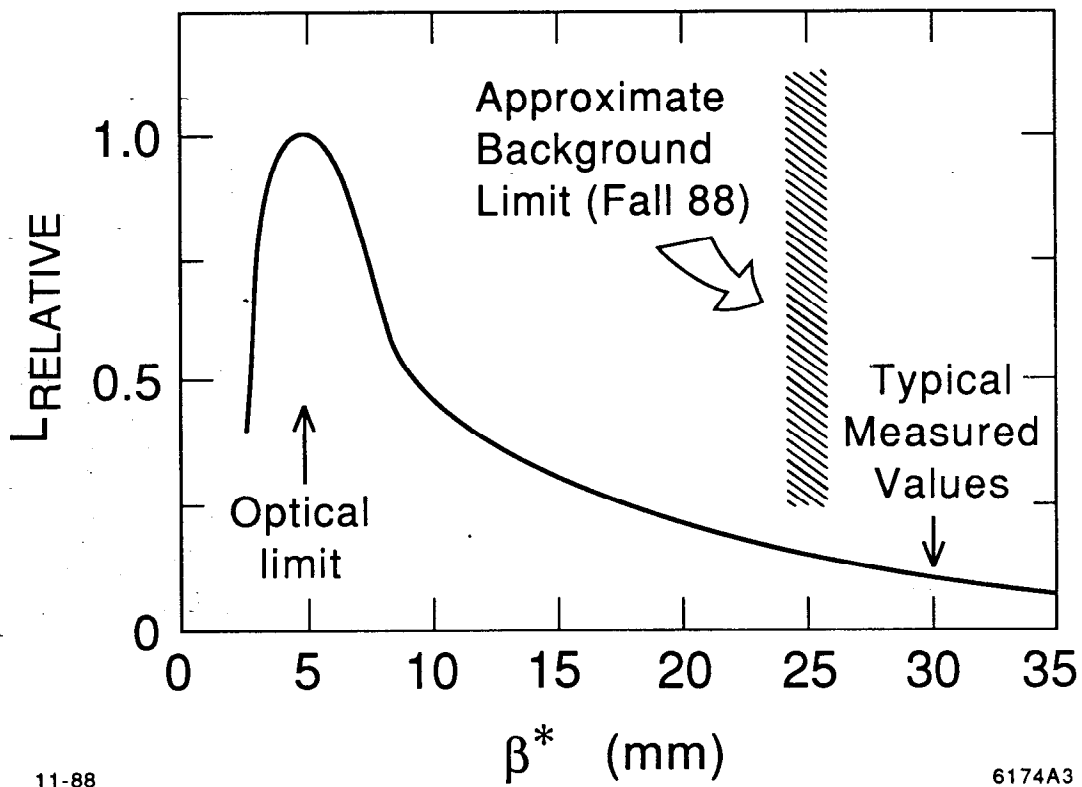


Fig. 2



11-88

6174A3

Fig. 3

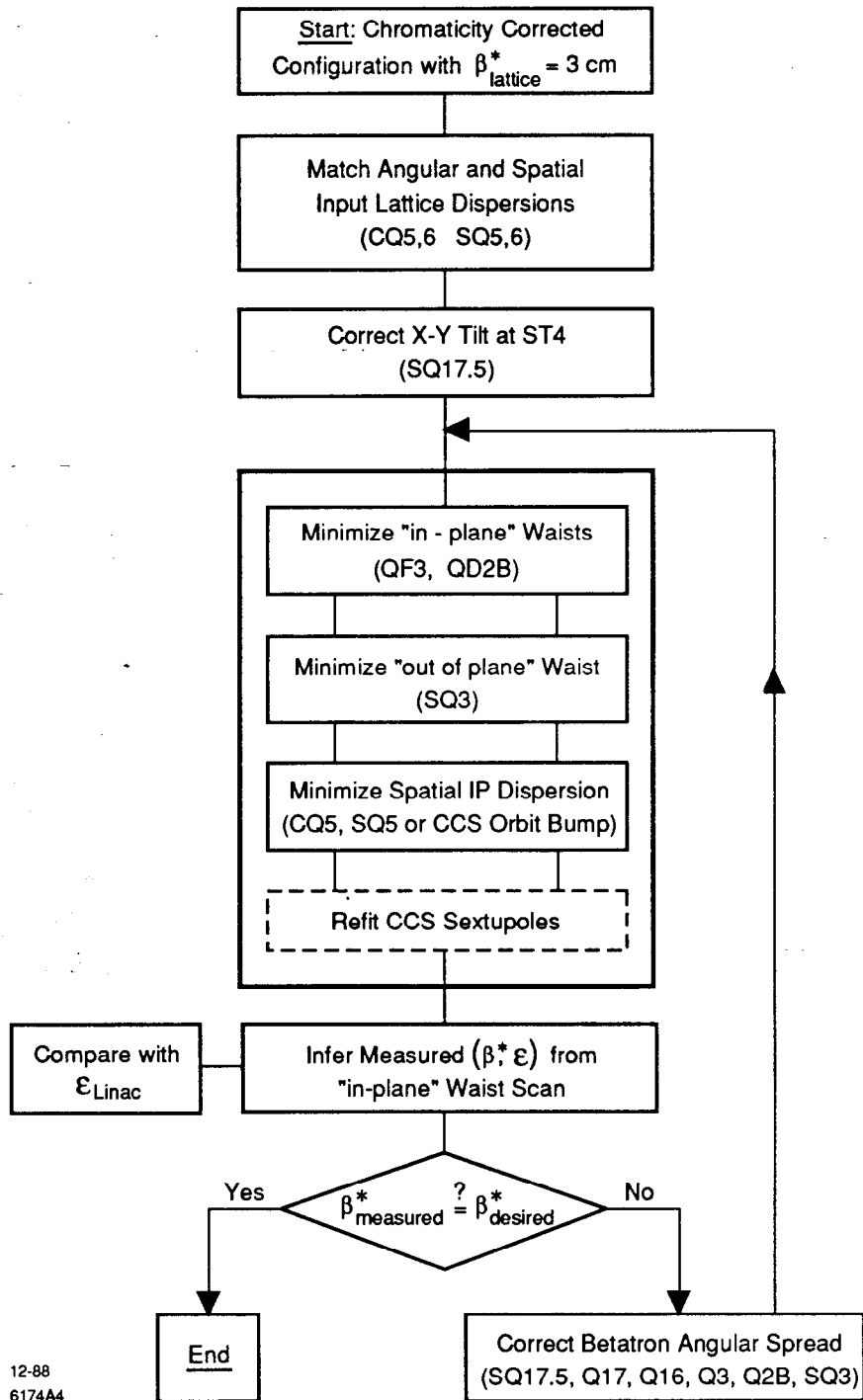
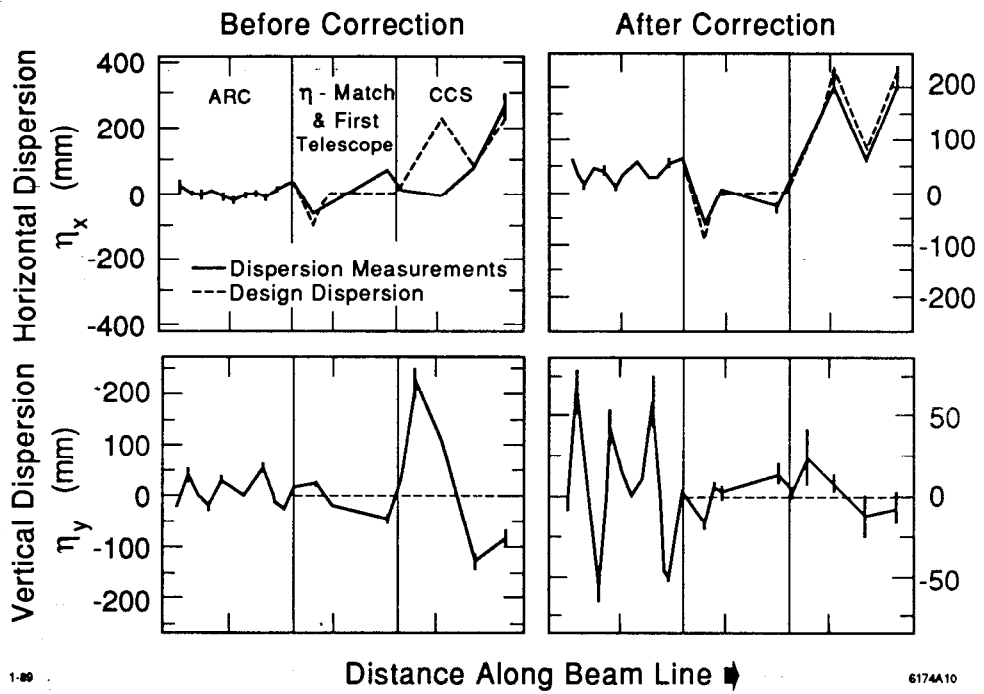


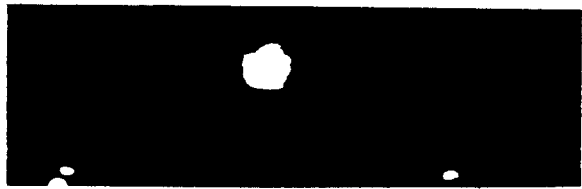
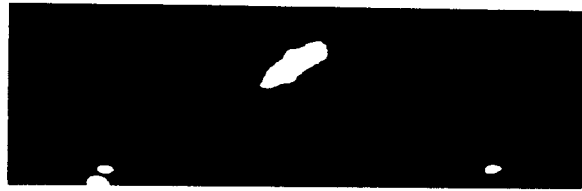
Fig. 4



6174A10

Fig. 5

|← cm →|



1-89

6009A14

Fig. 6

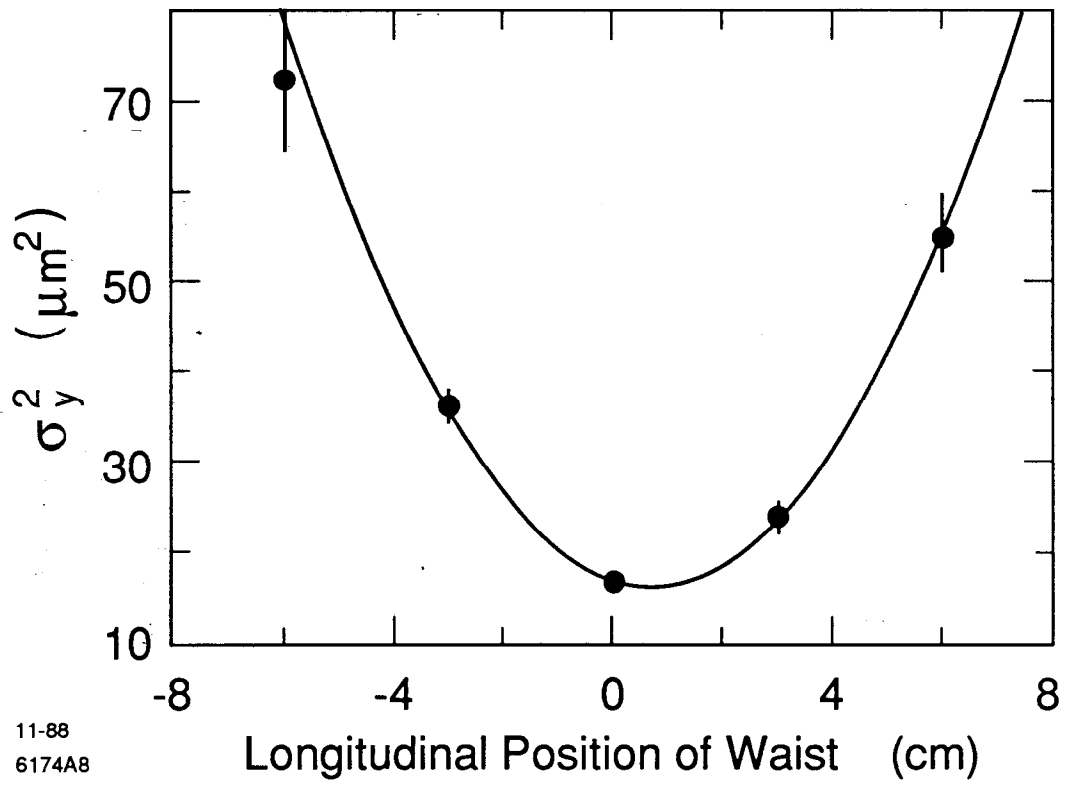
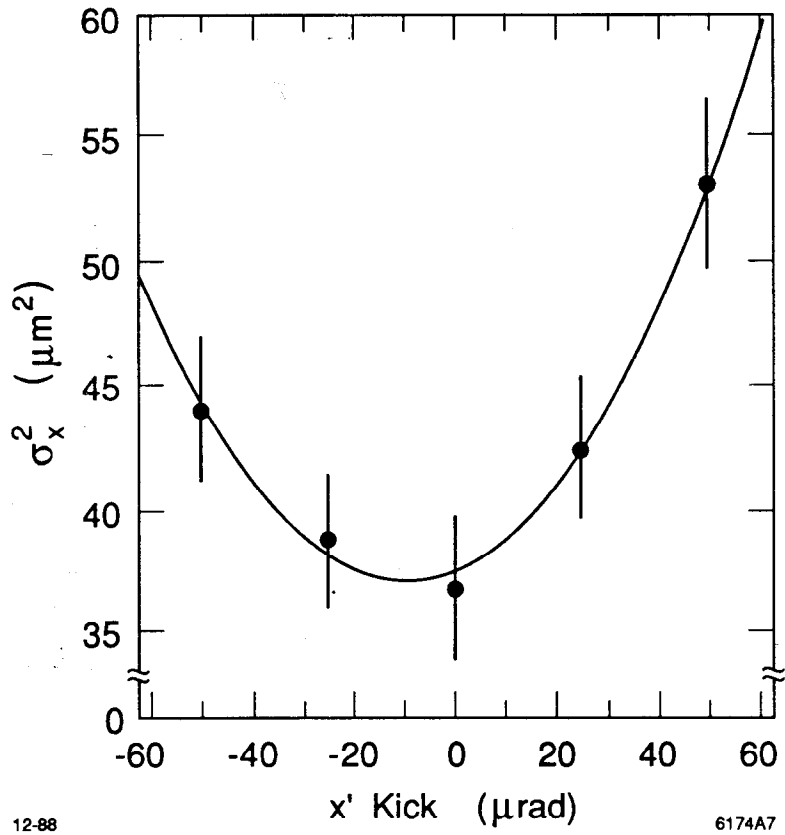


Fig. 7



12-88

6174A7

Fig. 8

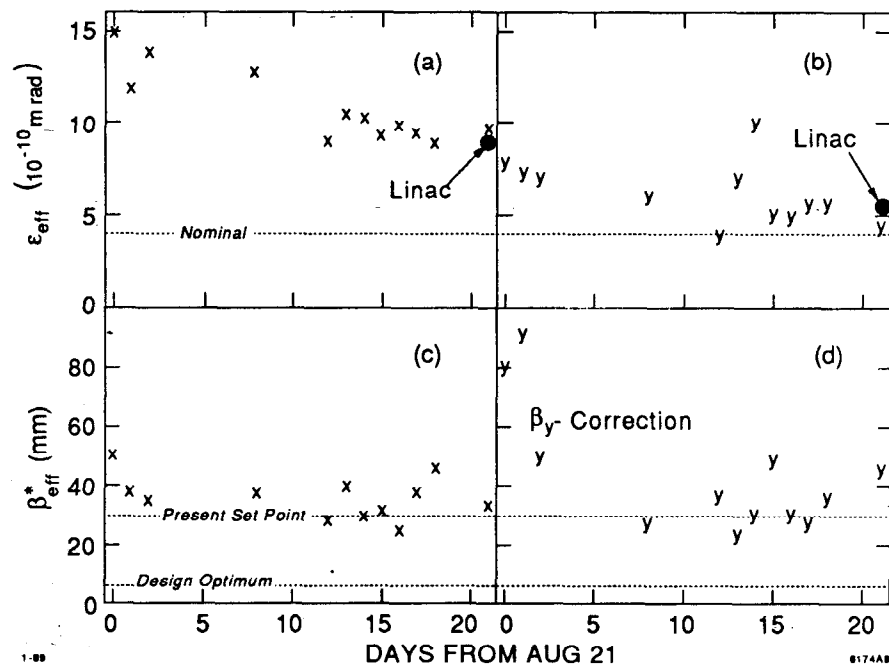


Fig. 9